COBEM 2023 27TH INTERNATIONAL CONGRESS OF MECHANICAL ENGINEERING

ABCM Brazilian Society of Mechanical Sciences and Engineering
27th ABCM International Congress of Mechanical Engineering
December 04-08, 2023, Florianópolis-SC, Brazil

COB-2023-1657
FLOW RATE MEASUREMENT OF TWO-PHASE FLOW IN DIFFERENT PATTERNS WITH A SINGLE THROTTLE DEVICE USING PgNN

Tiago F. B. Camargo
Centro de Ciências Exatas e Tecnológicas, Universidade Federal do Acre - BR 364, Km 04 - Distrito industrial-Rio Branco-AC
tiago.camargo@posgrad.ufsc.br
Emilio E. Paladino
Departamento de Engenharia Mecânica, Centro de Tecnologia, Universidade Federal de Santa Catarina EMC/CTC/UFSC Campus Reitor João David Ferreira Lima, s/nº Trindade – Florianópolis – SC Zip Code: 88040-900
emilio.paladino@ufsc.br

Abstract. *Typical flow rate correlations used in differential pressure flowmeters use the average $\overline{\Delta p}$ to correlate flow rate. The phase interactions as they flow through a constriction result in very specific characteristics of this signal. In this work, a deep learning model to develop a virtual flow sensor capable of determining individual phase flow rates from the transient differential pressure signal of a single throttle device. In addition, the proposed model considered some physical theories in learning. The inputs of the model are extracted from the time series of the differential pressure signal from a large dataset obtained from an experimental test of water-air horizontal flow that ranges from 0.03 to 1.10 m/s for liquid superficial velocity jl and 0.03 to 19 m/s for gas superficial velocity jg in a 25.4 mm internal diameter tube. The models based on PgNN and DNN were evaluated on another unseen orifice area ratio dataset to compare the performance and generalization of different learning methods.*

Keywords: *orifice plate , two-phase flow , two-phase flow metering , signal analysis , machine learning*

1. INTRODUCTION

The inline flow rate measurement of individual phases in gas-liquid two-phase flows is crucial for process monitoring and control in various industrial applications. Despite the availability of flow sensors capable of measuring the mixture mass or volume flow rate, another variable, such as phase volume fraction or slip velocity is necessary for the determination of individual phase flow rates. The sensors for the determination of phase fraction, as gamma-ray based or capacitive/resistive are complex, difficult to calibrate for large ranges of phase flow rates, and require specific protocols for their operation, which impedes their usage in harsh environments as deep offshore production. Another option, in the context of differential pressure based flow meters, is the use of two throttle devices, which, with the use of cross-correlated parameters allow the measurement of two flow variables. However, this approach again lacks generalization for large ranges of gas and liquid flow rates. However, there is a huge quantity of information in the transient Δp signal, mainly when it comes to gas-liquid flow streams. urthermore, although we use an orifice plate, the concept can be applied to any constriction available in the process that acts as a throttle device or a choke or flow control valve, since there is available data for model training.

The neural network, one of several machine learning techniques, finds increasing use in monitoring parameters that are difficult to measure directly. Therefore, it can perform the regression task with entries in the model of variables that are more easily measured in the phenomenon, which are influenced by the quantity to be measured. A multiphase flow meter elaborated by the technique of regression with machine learning is called in the literature as a virtual multiphase flow meter and is also known as soft sensor AL-Qutami *et al.* (2018); Hansen *et al.* (2019). The application of machine learning in the determination of flow regimes and phase velocity is initially addressed by Beg and Toral (1993) with signal analysis and pattern recognition technique that aims to categorize images or data sets. These extract and identify stochastic attributes making it possible to obtain a two-phase flow meter through software. In a work by the same group, Cai and Toral (1993) used pattern recognition maps to determine flow regimes and neural networks to estimate phase velocities, with these tools he sought a model to obtain both flow pattern and individual velocity of each phase with 10% accuracy. These two works were carried out in the same configuration where the pressure fluctuation signal was taken from a differential pressure gauge in an orifice plate with horizontal flow. Other works used a Venturi tube and differential pressure gauge Minemura *et al.* (1998); Wang *et al.* (2020). The work by Wang *et al.* (2020) reports the use of a differential pressure gauge in two sections, the contraction section and the expansion section. The study by Shaban and Tavoularis (2014) does not use restriction, but only the measurement of the differential pressure transient signal between two close points in a straight vertical tube, to obtain phase velocities with estimators modeled in machine learning. The author uses the PDF of the pressure differential signal as input attributes of the neural network. Xie *et al.* (2004) use spectrum of pressure differential signal as artificial neural network input attributes to point out the type of pattern in gas-liquid-fiber

multiphase flow.

The works on soft sensor two-phase flow meters found in the literature do not use mechanistic models based on physics in the inputs. Thus, there is an opportunity to investigate the use of concepts and physical models to improve the generalization of models made in machine learning. Other problems, not addressing flow meters, as described by Kanin *et al.* (2019), are found some physical input concepts in the elaboration of the prediction method. Another opportunity is to guide training through loss functions by applying physically consistent constraint Karpatne *et al.* (2017).

The knowledge of physical models consolidated in the literature is not being used in studies using machine learning to determine phase throughput, which makes the output model very dependent on the training data. This fact with those previously mentioned motivate to seek greater generalization of the models using machine learning by inserting physics in the model.

2. Physics-guided Neural Network

Studies in data sciences and machine learning seek the generalization of the estimator for a given task. Regularization and DANN (Ganin *et al.*, 2016) are examples of this path. In recent years, the limitations of machine-learned estimators have become more evident in the desire to use them in any and all situations. As far as generalization is concerned, the standard techniques use available data and are accurate where there is enough data. In engineering applications, we often want to know phenomena where there is no data or very little of it. A classic example is the problem of determining the trajectory of the cannonball, where the estimator must trace the trajectory of the bullet with only initial data of its ascent, whose training of the regression function, consequently, can occur up to half of the trajectory to be traveled. The estimator will do its job well until the halfway point, the climb, but it will not predict for example where the bullet will land due to lack of data to train the model. The physical concepts and classical formulations in the problem are already well known. The crash site is very well predicted knowing from initial data. In another situation, such as multiphase flows, however, it is very difficult to accurately model the phenomenon with existing physical models. In this way, combining machine learning with existing knowledge of physics has the opportunity to improve estimators to perform a certain task that encompasses more complex physical phenomena.

The first attempt to include the physics of the phenomenon to machine learning is to propose the input of the neural network with one or more attributes from a physical model. However, avoiding coefficients and empirical corrections so that deviations from reality are corrected by neural networks. Feeding a physics-based model is a simple approach, but it already adds physical attributes to the system. This can be verified through the value of the gradients obtained from the operation of differentiating the input sequences (Goh, 1995; Zhang *et al.*, 2018). The higher the average gradients, the greater the attribute's impact on the final prediction. The initialization of the weights related to the information path of the physical model attribute can be set to maximum to increase relevance already at the beginning of training, finding gradient minimums close to a higher weight in this input.

At the beginning of the training, alternatively, it is interesting to carry out a pre-training with the target outputs of the theoretical model itself in case of not using outputs with the proposed objective, in this case, liquid and gas flows. The pre-training with synthetic values tends to implant in the network a non-linear function similar to the formulation itself with physical concepts, getting closer to the theoretical values where there are few data, since synthetic data from theoretical models can have many points for training (Jia *et al.*, 2021; Shah *et al.*, 2018).

Knowledge of the physics of the phenomenon is possible to be used both in the input and output of the neural network. Specifically, the network output loss function can be modified by adding a physics influence or laws residuals Daw *et al.* (2021); Raissi *et al.* (2017). Raissi *et al.* (2017) reports how partial differential equations can be solved and presents examples with Burger and Shrödinger equations through machine learning called Physics-informed Neural Network. Other authors Xiang *et al.* (2021) following this line, present the application of residuals mentioned by Raissi *et al.* (2017) in a more comprehensive way for equating the movement of fluids, however, with an attempt to better calibrate the exchange of information with physics through a noise parameter. The architecture and objectives may be different in a specific problem, it may be necessary to directly apply fundamental equations, use physical limitations or address consolidated correlations in the literature, as is the flow measurement with a restriction addressed in this text. Applied problems have specific physical concepts as in the work of Daw *et al.* (2021) who tackles the problem of predicting the water temperature of reservoirs according to depth. In this work the model is elaborated by means of a constriction with the density property that respects physics. The generic equation for applying physics to the loss function is shown below (Karpatne *et al.*, 2017),

$$\text{Loss} = \text{Loss}_{\text{train}}\left(Y_{\text{truth}}, \hat{Y}_{\text{train}}\right) + \lambda R(W) + \gamma\, \text{Loss}_{\text{PHY}}\left(\hat{Y}_{\text{train}}\right) \tag{1}$$

The conventional form for the loss function is the training error Loss_{TRN} between true Y_{truth} and predicted Y_{train} , the regularization term $R(W)$ with its exchange coefficient λ. To guide the training of a model with physical consistency, an existing physical constraint in the phenomenon Loss_{PHY} is added, the hyperparameter γ determines the relevance in the

information exchange. These values are the object of studies to improve learning. A very strong physical constraint turns the influence of the physical model into an authoritative one. It is proposed to use a model already known in multiphase meters as input to the neural network. Also, as a possible proposal, the implementation of a loss function including physical consistencies.

3. METHODOLOGY

The temporal series of differential pressure of an experimental bench is used the relate the flow behavior to a transient signature from the signal. The experimental procedure operates ranges of 0.03 to 1.17 m/s liquid superficial velocity j_l and 0.03 to 19 m/s gas superficial velocity j_g on a horizontal configuration of a 25.4 mm internal diameter. The flow pattern of each pair taken by photograph 15D and visual observation through transparent acrylic upstream of the orifice plate was disposed on a flow pattern map. The test section used to take difference pressure fluctuations was mounted horizontally, and comprised a plate of 3 mm with square edges orifice of 12.7 mm. It is distant 25.4 mm from the taps on each side of the plate. The development upstream section was 12.5 m long, and the mixture was discharged into a separated tank 1.6 m from the orifice plate.

Two quantities of pressure fluctuations were used to observe the characteristics parameters from the samples of 119.7 s each collected at 1000 Hz. One is differential pressure signal Δp and another normalized pressure fluctuation in the times series, then the signal variance is one. The use of the mean of samples purposes centering the distribution for the PDF representation in this text, it is more useful to use the mean of one sample when it is supposed for unknown samples of a wide range of superficial velocity. Two pattern flow maps is shown in Fig. 1 to basis condition of flow identification. The regimes patterns maps where conceived to identify flow structures which can impact pressure loss and heat exchange.

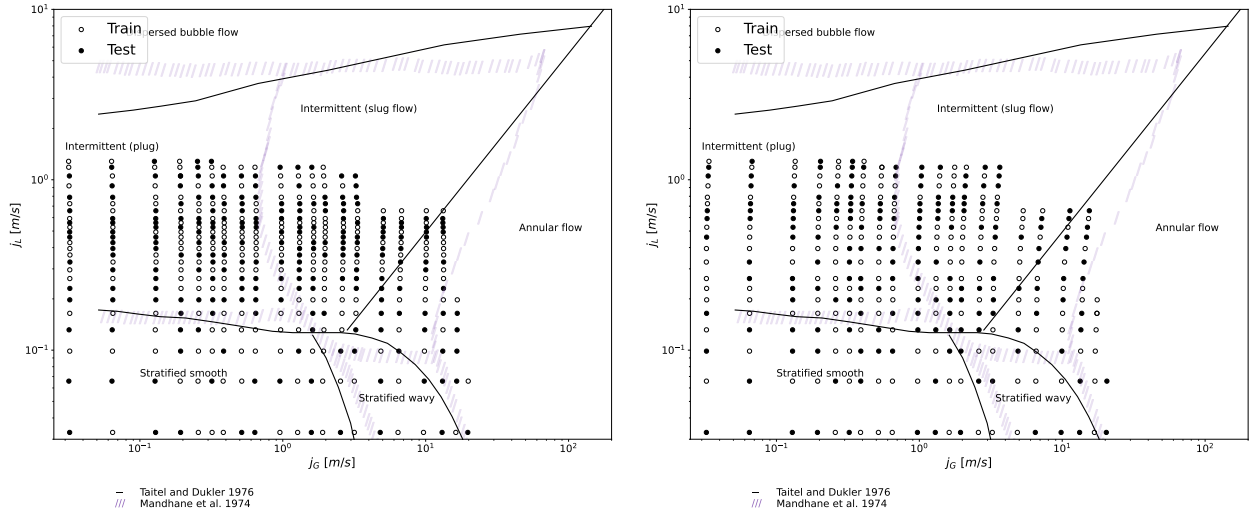

(a) 0.5 (b) 0.74

Figure 1: Conditions of flow tested. The flow conditions investigated in this study were plotted against Taitel and Dukler (1976) and Mandhane *et al.* (1974) for two orifices diameter ratio 0.50 and 0.74. There is some names to describe flow regime and the common used in horizontal flow is plug, stratified smooth, wavy, annular, slug and bubbly.

3.1 Network input estimation based on process physics

The mean differential pressure is commonly used as input for machine learning models. Although it offers a primary and very related feature with flow rate of phases, it can be disadvantageous when seek generalization. The differential pressure is a function of geometry of orifice. The increase of velocity in restriction cause most part of this differential pressure. Another part is the permanent loss pressure also dependent of orifice geometry. This input can be pass by a physical function, or filter, to surpass the problem of feature geometry dependency. In this study is assumed as an estimate to use as input, the mass rate flow can be used for each phase flowing in area αA for gas and $(1-\alpha)A$ for liquid where α is gas fraction (Murdock, 1962),

$$\tilde{\dot{m}}_l = \frac{(1-\alpha)AC_d}{\sqrt{1-\beta^4}}\sqrt{2\Delta P_{tp}\rho_l} \qquad ; \; \tilde{\dot{m}}_g = \frac{\alpha A\epsilon_g C_d}{\sqrt{1-\beta^4}}\sqrt{2\Delta P_{tp}\rho_g} \tag{2}$$

where ρ and ϵ_g is obtained with ideal gas relations from measured inlet pressure, β is orifice to pipe diameter ratio. The gas fraction is unknown. The scheme is to encode the gas volume fraction $\tilde{\alpha}$ as part of the network. This not aim

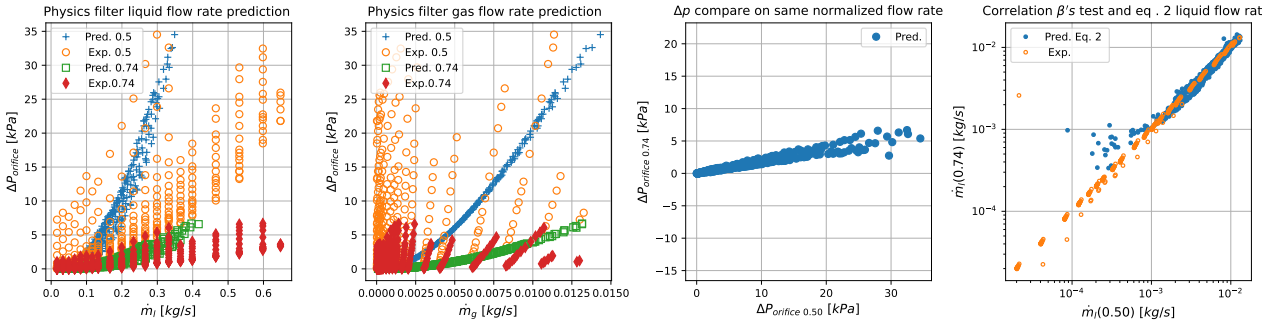

Figure 2: Evaluation of correlation of predict flow rate using Equation 2 with constant α=0.5

obtain truly α, but impose some physical relation. This parameter is shown comparatively to α from correlation. This $\tilde{\alpha}$ is gradients dependent modeled with a *sigmoid* activation function, the pass of this function value assume to represent the gas fraction. In this work the first option is used allowing the network use Eq. (4) as a filter for the Δp feature input. Although the deep neural network uses the physical input as an attribute, and as such is subject to calibration by means of weights, the author seeks an input with the best possible physical sense for the entire flow rate tested.

The model can avail the knowledge already provided on literature to guide resultant output using correlation for two-phase flow proprieties. The two phase differential pressure acquire experimentally is compared with calculation of a estimated $\Delta\hat{p}_{tp}$ which among literature correlations for orifice plate Chrisholm (1977) count for slip velocity. As geometry changes the contract section area, this should be considerate. Correlation uses the balance of forces and considers the shear forces between phases that are relevant to the pressure gradient determination, given by,

$$\phi_{\mathrm{lo}}^2 = 1 + \left(\frac{\rho_l}{\rho_g} - 1\right)\left[B\mathrm{x}(1-\mathrm{x}) + \mathrm{x}^2\right] \tag{3}$$

where B for thin plate holes,

$$B = \frac{\left[\frac{1}{(C_c\sigma)^2} - 1\right]\frac{1}{S} - \frac{2}{C_c\sigma S} + \frac{2}{S^{0.28}}}{\frac{1}{(C_c\sigma)^2} - 1 - \frac{2}{C_c\sigma} + 2} \tag{4}$$

where C_c is coefficient of contraction shown in next section, S the slip velocity ratio between phases and σ is the cross section ratio of orifice plate. Then can find two-phase gradient $\Delta p_{tp} = \phi_{LO}^2 \times \Delta p_{LO}$, where lo means total mass flow as liquid. The gas fraction is not easily obtained, requiring specific sensors, but there are correlations to determine it that can be applied (Gardenghi *et al.*, 2020). The study by Lockhart and Martinelli (1949) presents a correlation for horizontal flow of diameters from 1.5 mm to 25.4 mm expressed by,

$$\alpha = \left[1 + 0.28\left(\frac{1-\mathrm{x}}{\mathrm{x}}\right)^{0.64}\left(\frac{\rho_g}{\rho_l}\right)^{0.36}\left(\frac{\mu_l}{\mu_g}\right)^{0.07}\right]^{-1} \tag{5}$$

In order to propose an estimate of phase flows for the input of the neural network in the entire flow range, transient characteristics were used, in addition to the average differential pressure. The PSD, PDF and DWT distributions were used, and characteristics derived from them as mean, first, second, third, forth moments from PDF,frequency of peak and peaks from PSD. Briefly, there is a total os 211 features taken from transient differential pressure signal, 60 from PSD up to 10 Hz, 60 from PDF, 64 from DWT and 27 signal characteristics. A selection was elaborated using Person correlation and linear least squares.

3.2 Proposed formulation for training error update

The error during training is conventionally done with the terms mean squared error and the regularization term. The last seek generalization of output. The proposal is to take along with the $Loss$ error physical consistencies of the two-phase flow phenomenon in the imposed restriction. The neural network below presents the estimated output for flow rates of phases $\hat{\dot{m}}_l$ and $\hat{\dot{m}}_g$, to train this network resort to the algorithm of *gradient descent* which uses the error between estimated and true value. With this network output it is possible to obtain a mass fraction, $\hat{\mathrm{x}}$ as shown in the Fig. 3.

The function loss physics based can be elaborated by the physical lower limit of Δp_{tp}, in which the permanent pressure drop in the orifice only with mass gas flow, $\Delta p_{g\ net}$, and added to the permanent pressure drop of the liquid alone $\Delta p_{l\ net}$

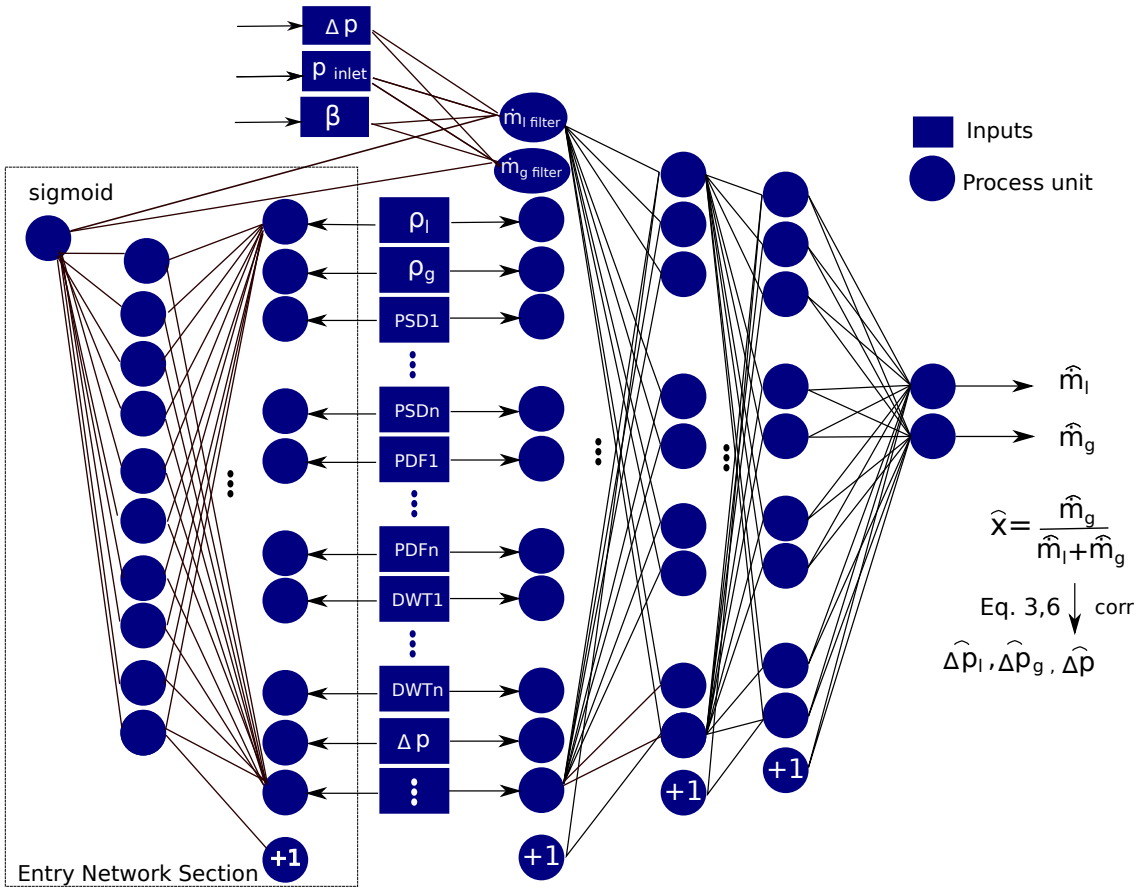

Figure 3: Neural network with proposed inputs and outputs.

flowing, it is not possible to be less than the pressure drop between the pressure taps with the two flows together in two-phase flow.Assuming that $\sigma = \beta^2$ and $C_c = A_c/A_D\sigma$, the head loss for the orifice plate is given by,

$$\Delta p_{\text{net sigle-phase}} = \frac{1}{2}\rho V_1^2 \left(1 - \left(\frac{1}{C_c\sigma}\right)\right)^2 \tag{6}$$

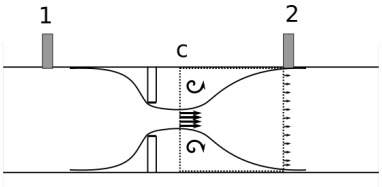

Figure 4: Control volume after orifice plate

The coefficient of contraction is still an unknown term. The author Chrisholm (1984) presents the contraction coefficient for liquid or gas flow in the duct based on the study by Jobson (1955), for liquid flow he provides the correlation for the contraction coefficient, given by,

$$C_c = \frac{1}{[0.639(1-\beta)^{0.5} + 1]} \tag{7}$$

Equation (7) correlation is used in Eq. (6) to determine the flow resistance subject to the orifice plate, i.e. from inlet to pressure recovery to obtain the estimated pressure drop, Eq. (6) was used with the estimated values $\hat{\dot{m}}_l$ and $\hat{\dot{m}}_g$. Figure 5 presents evidence of the difference between the pressure drop for the two-phase experimental test for various flows and that calculated by Eq. (6) with the experimental mass flows using $\Delta p_{g\ net} + \Delta p_{l\ net}$ of gas and liquid alone flowing.

$\Delta p_{g\ net}$ is calculated with the mass flow rate of the gas flowing alone for A, so the local velocity U_g is smaller in relation to the two-phase flow in which the gas theoretically flows on average for $A\alpha$. For $\Delta p_{l\ net}$, likewise, U_l flows through A, but for Δp_{tp} it flows through area $A(1-\alpha)$. As the velocity is lower, the pressure drop is lower for the flow of the phases alone in the pipe, in a simple analysis of the order of magnitude $\Delta p \sim (j_l + j_g)^2$ is greater than $\Delta p_g + \Delta p_l \sim j_l^2 + j_g^2$.

Pressures above the sum of $\Delta p_{l\ net} + \Delta p_{g\ net}$ must be the limit given by physics, so the formulation can be done as expressed in 8 .

$$Loss1_{\text{PHY}} = \sum_{j=0}^{M} \left(ReLU \left(\left(\Delta p_{spl} \left(\hat{m_l}_j \right) + \Delta p_{spg} \left(\hat{m_g}_j \right) \right) - \overline{\Delta p_{tp\ j}} \right) \right) \tag{8}$$

where $\overline{\Delta p_{tp}}$ is the average pressure differential obtained from the orifice plate, Δp_{spl} and Δp_{spl} pressures calculated with the estimated mass flows, M number of examples, using gradient descent, or number of errors used, in the case of using stochastic gradient descent or other batch error update.

Another proposal is to add to the $Loss_{\text{PHY}}$ the error in relation to the literature correlations, in this formulation the error is bilateral, it can assume negative and positive values resulting in a strong physical constriction. With this, it is interesting to use a coefficient ζ de to regulate its influence, its value can be later optimized with other techniques to determine better training hyperparameters. The mass fraction $\hat{\text{x}}$ is obtained with the values of $\hat{m}_l$ and $\hat{m}_g$. With the correlations from Chrisholm (1977) of the two-phase multiplier $\Delta\hat{p}_{tp}$ is obtained and the error formulated with Eq. (9) using ReLU modified, $f(z) = max(0, z-b)$ where b is the intercept value, best shown in Eq.. (**??**). This value is determined by the expected maximum error $E_{\text{max}}\Delta p_{\text{correlation}}$ that the pressure drop correlation can provide. In Fig. 5c a scheme is presented in which points the error of formulation based on physics would influence, the zone between the dotted lines has the objective of not having an effect due to the uncertainty of the correlation itself, outside of which the $Loss2_{\text{PHY}}$ would act to guide the training.

$$Loss2_{\text{PHY}} = \sum_{j=0}^{M} \text{ReLU} \left[0; \left\| \left(\Delta\hat{p}_{tp_j} \left(\hat{m}_l; \hat{m}_g \right)_j - \overline{\Delta p_{tp_j}} \right) \right\| - E_{\text{máx.corr}} \overline{\Delta p_{tp_j}} \right] / \overline{\Delta p_{tp_j}} \tag{9}$$

So,

$$Loss_{\text{PHY}} = \gamma\, \text{Loss1}_{\text{PHY}} \left(\hat{m}_l; \hat{m}_g; \overline{\Delta p_{tp}} \right) + \zeta\, \text{Loss2}_{\text{PHY}} \left(\hat{m}_l; \hat{m}_g; \overline{\Delta p_{tp}} \right) \tag{10}$$

So the training error can be expressed by the following,

$$Loss = \text{MSE}_{\text{train}} + \lambda R_W(\boldsymbol{w}) + \text{Loss}_{\text{PHY}} \tag{11}$$

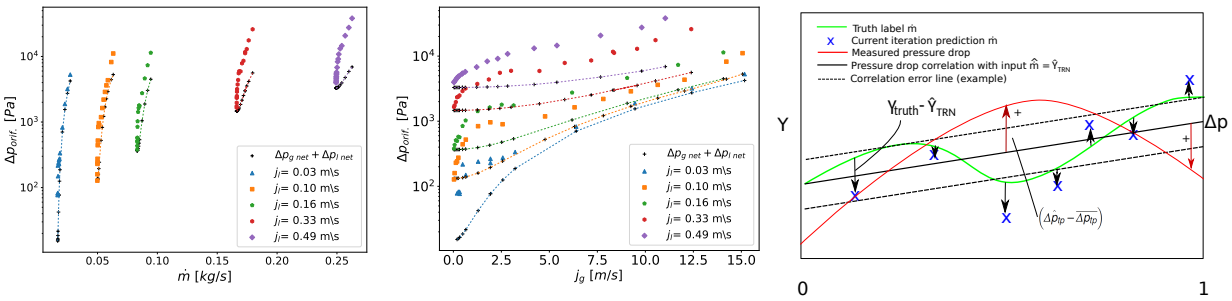

(a) (b) (c)

Figure 5: Two-phase test pressures along with the calculation of $\Delta p_{\text{net l}} + \Delta p_{\text{net g}}$ (a,b). Training error and correlation error scheme, arrows in red and black, respectively, physics theory correlation and training error (c).

The last physics theory where encoded as part of the net using a processing unit with sigmoid activation function and one neuron, resulting in a value between 0 and 1, similar limits values of the gas fraction. The input layer feeds the network connected with the 'physical filter' results in a guess mass gas and liquid rate. This information is forward to a network that is also fed with the same input layer. The information about the first network was put as the needed value

for α described in Eq. (4). During training, the dynamic mass fraction $\tilde{x}$ is evaluated with final $\hat{x}$ calculated by the mass rate predicted from whole network on the last layer. The figure 3 shows neuron with a sigmoid activation connection to the physics filter process unit. On backpropagation, this error is also evaluated and the whole net weights are updated.

The network architecture was the following for the entry section network: 128 neurons, batch normalization, dropout of 10%,64 neurons, batch normalization, dropout of 10% and one neuron layer using weight regularization. The principal right network used the same sequence neurons with regularization, batchnormalization, dropout of 10% layers, comprising 5 neurons layers of 215, 512, 256, 128, and 32 units of hidden layer and two exponential output units. The regularization L2 norm term λ is used with a high value, which may give a higher error but more generality. The DNN architecture is the same but does not use the entry network section as detached in Fig. 3.

Finally, the activation function, batch size, coefficients γ and ζ, and E_{max} were tuned with algorithm Bayesian Optimization. The author choose tune E_{max} than test the correlation errors, but a analysis is determine this percentage error for more geometries. In addiction, the truth value against correlation is already been evaluated during hyperparameters optimization. A five Fold cross validation were perform in each iteration the test accuracy done with remain training dataset. A unseen test data was not used in training either coefficients optimization for final test of predictions. The results prediction of α recursively calibrated as part of network were learning or weight transferred for a model as only same structure respective network of it. Then, a separated net with trained weights used to obtain $\tilde{\alpha}$. The evaluation is made by Mean Squared Error (MSE) and Mean Absolute Percentage Error (MAPE) as described in Tab. 1 using a 4-Fold.

Table 1: Error description evaluated for models and geometries.

ID of Error	Evaluation description
Error 1 liquid	net trained on β=0.5 evaluated on β=0.5 MSE mass liquid rate
Error 2 liquid	net trained on β=0.5 evaluated on β=0.74 MSE mass liquid rate
Error 1 gas	net trained on β=0.5 evaluated on β=0.5 MSE mass gas rate
Error 2 gas	net trained on β=0.5 evaluated on β=0.74 MSE mass gas rate
Error 1 %	net trained on β=0.5 evaluated on β=0.5 MAPE liquid and gas
Error 2 %	net trained on β=0.5 evaluated on β=0.74 MAPE liquid and gas
PgNN 1 and DNN 1	Inputs of characteristics and distributions PDF, PSD and DWT
PgNN 2 and DNN 2	Inputs of characteristics
PgNN 3 and DNN 3	Inputs of PgNN 1/DNN 1 features ρ_{xy} and bias criteria selected

4. RESULTS AND DISCUSSION

A evidence of generalization in the model with physical guide learning is test two geometries of orifice plate. The training occurs in a geometry and evaluate the error of prediction in a distinct orifice area ratio for a DNN and described PgNN. Other analysis is select the characteristics of the signal that less change with the geometry and train the model then predict with test data. A three steps cross-validation is done and extracted the standard deviation and mean error to compare the models.

The results can be shown in a plot comparing truth and prediction of the PgNN described. On the Fig. 6 are results of training on geometry with β=0.5, where MSE of test set is 1.44 kg^2/min^2 for liquid flow rate. This trained network was also predicted the flow rates from data of other geometry with β=0.74. A agreement with true values is seen on low liquid flow rates and average gas flow rates. This prediction results in a MSE of 11.11 kg^2/min^2.

The $\tilde{\alpha}$ is shown in Fig. 6a in red. This were passively trained with results of $\tilde{x}$ obtained from 4 compared to $\hat{x}$ summing their RMSE in overall error. So this will be calibrated by their own prediction of phases flow rate. In the plot we compared the output of this α portion of network with a correlation of literature that use x from measured phases flow rate and the x itself. It shows high variability and values lower than correlation higher than measured x. A complete evaluation may compare with experimental α. Although the difference from correlation, this training and learning transfer can be as a way of estimate gas fraction using data from mass flow rate and pressure through a orifice plate.

The process of training considering the physics was evaluated with different dataset from the same time series as can be seen on Tab. 2. The conception of error shown in this table was to investigate the accuracy on geometry trained same of tested, and also verify the error predicting a much different area ratio. This aim to understand the generally property of inputs used with PgNN and DNN, in the same manner the two NN's against each other. Noting that the inputs were preprocessed focusing to be normalized, seeking to extract the signature of signal, then trying to avoid dependency with geometry.

The liquid flow rate shows always less errors for network type and input tested as seen in Fig. 6. The procedure of cross-validation for four splits results in the performance from Tab. 2. The error of PgNN is close to DNN using the dataset of all inputs when predicting the condition on same geometry. The estimated values of mass flow rate of phases trained in

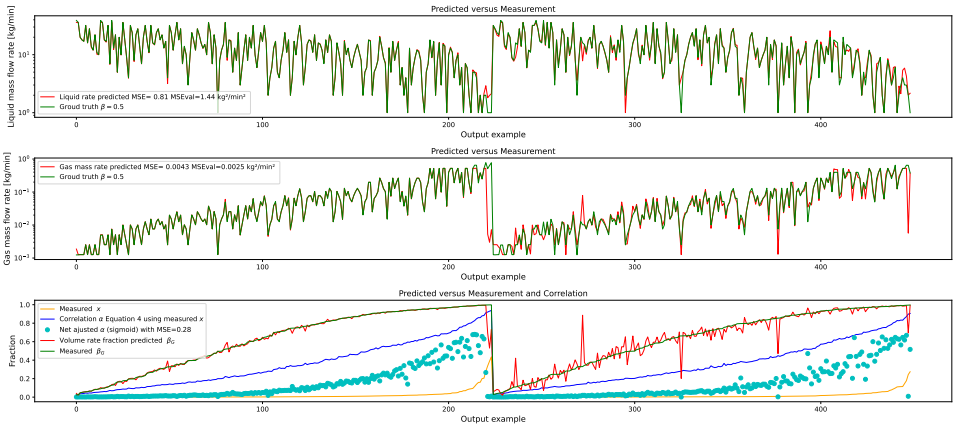

(a) Orifice Trained β=0.5. The half left portion is prediction on train data, right is test data. Model trained using PgNN proposed.

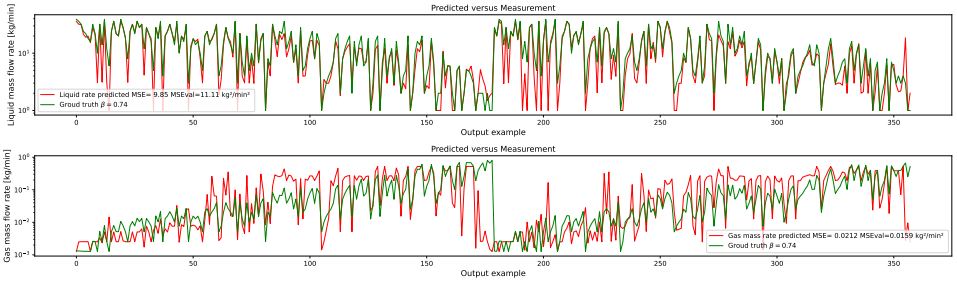

(b) Orifice Tested β=0.74. Prediction on test data. Model trained using PgNN proposed.

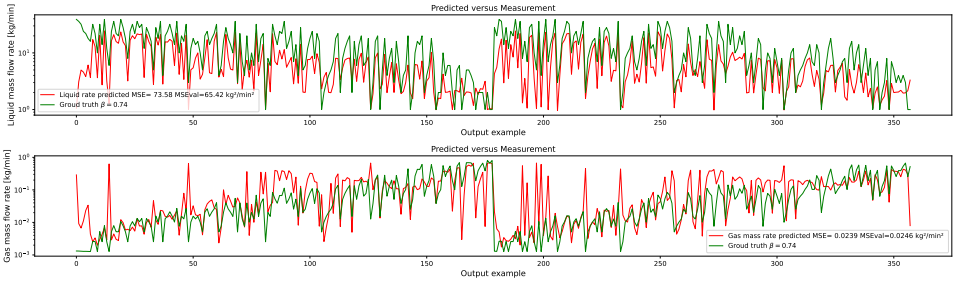

(c) Orifice tested β=0.74. Prediction on test data. Model trained using DNN.

Figure 6: Two-phase differential pressures $j = 0, 1, ..M$ output examples along with the calculation of correlation $\Delta p_{tp}\left(\dot{m}_l; \dot{m}_g\right)_j$ truth gas and liquid rate.

.

Table 2: Cross-validated models evaluation with 4 train-validation dataset splits.

Error	PgNN 1	PgNN 2	PgNN 3	DNN 1	DNN 2	DNN 3
Error 1 liquid	5.96	13.85	10.05	7.64	3.11	8.37
Error 2 liquid	30.60	52.81	32.99	84.68	127.16	34.48
Error 1 gas	0.0168	0.0189	0.0151	0.0086	0.0047	0.0074
Error 2 gas	0.0297	0.0302	0.0303	0.0276	0.0485	0.0301
Error 1 %	27.41	33.36	33.46	23.99	36.34	27.97
Error 2 %	82.96	79.56	78.03	489.31	577.90	115.50

one geometry and testing in another shows a little better performance for Error 2 using PgNN. Observing the MSE metric for gas mass rate there is any changes or tendency in performance using the features set either networks evaluated. This difference can be due to the correlation used as seen in Fig. 7. The Δp predict by correlation using measured $\dot{m}_g$ and $\dot{m}_l$ was plot showing that it do not fit well on β=0.74 orifice for low pressures.

The gas flow rate prediction have problem to fit in high gas volumetric rate fraction β_G as shown in Fig. 6a. Mainly this issue arise because the close form of distribution and features in two region of the flow map chart. Most cases occurs similar features in wavy and bubbly regions. Also, the pressure drop for low liquid flow rate is near the lower limit

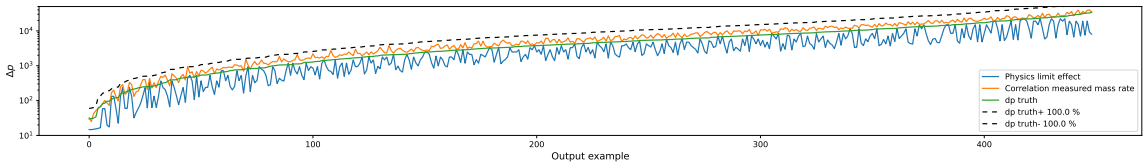

(a) β=0.50

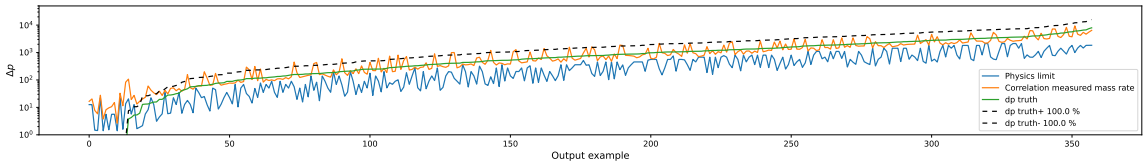

(b) β=0.74

Figure 7: Two-phase differential pressures $j = 0, 1, ..M$ output examples along with the calculation of correlation $\Delta\hat{p}_{tp}\left(\dot{m}_l; \dot{m}_g\right)_j$ truth gas and liquid rate

of differential pressure transducer rising the error as can be seen in Fig. 7 at the low differential pressure. Finally, the contained liquid upstream orifice offers a hydrostatic differential pressure higher then other dynamic force described in literature correlation.

5. CONCLUSION

The characteristics and distributions shown and analyzed in this text highlight features that can be used in machine learning methods such as neural networks. They can estimate the flow rate of phases under the studied range conditions. The results can be improved with lower regularization term influence for the same geometry to less than half showed. In the high gas fraction range, it shows a poor performance prediction for the gas phase flow rate. The proposed PgNN was compared with DNN, and the results were evaluated. The errors for models tested in the same geometry are similar to each other, but the PgNN avoids overfitting, which causes extreme high outliers predictions in the test dataset moving the training toward physical consistent estimation. The physical considerations in the neural network impact the error when other geometry is tested for the architecture used and features set showed . The geometries studied are very different, other cases of minor changes in the orifice ratio are expected to have better results. The inputs features set can impact the metrics to not generalize model on other geometry, specially the gas phase whose lower density difficult the sensibility related to the features inputs and consequently during training. Further input features extraction methods or sets needs evaluation to clarify the investigation.

6. REFERENCES

AL-Qutami, T.A., Ibrahim, R., Ismail, I. and Ishak, M.A., 2018. "Virtual multiphase flow metering using diverse neural network ensemble and adaptive simulated annealing". *Expert Systems with Applications*, Vol. 93, pp. 72–85. ISSN 0957-4174. doi:https://doi.org/10.1016/j.eswa.2017.10.014. URL `https://www.sciencedirect.com/science/article/pii/S0957417417306875`.

Beg, N. and Toral, H., 1993. "Off-site calibration of a two-phase pattern recognition flowmeter". *International Journal of Multiphase Flow*, Vol. 19, pp. 999–1012.

Cai, S. and Toral, H., 1993. "Flow rate measurement in air-water horizontal pipeline by neural networks". In *Proceedings of 1993 International Conference on Neural Networks (IJCNN-93-Nagoya, Japan)*. Vol. 2, pp. 2013–2016 vol.2. doi: 10.1109/IJCNN.1993.717053.

Chrisholm, D., 1977. "Research note: Two-phase flow through sharp-edged orifices". *Journal of Mechanical Engineering Science*, Vol. 19, No. 3, pp. 128–130.

Chrisholm, D., 1984. "Measuring techniques in gas-liquid two-phase flows". doi:10.1007/978-3-642-82112-7.

Daw, A., Karpatne, A., Watkins, W., Read, J. and Kumar, V., 2021. "Physics-guided neural networks (pgnn): An application in lake temperature modeling".

Ganin, Y., Ustinova, E., Ajakan, H., Germain, P., Larochelle, H., Laviolette, F., March, M. and Lempitsky, V., 2016. "Domain-adversarial training of neural networks". *Journal of Machine Learning Research*, Vol. 17, No. 59, pp. 1–35. URL `http://jmlr.org/papers/v17/15-239.html`.

Gardenghi, A.R., Filho, E.d.S., Chagas, D.G., Scagnolatto, G., Oliveira, R.M. and Tibirica, C.B., 2020. "Overview of void fraction measurement techniques, databases and correlations for two-phase flow in small diameter channels". *Fluids*, Vol. 5, No. 4. ISSN 2311-5521. doi:10.3390/fluids5040216. URL `https://www.mdpi.com/2311-5521/5/4/216`.

Goh, A., 1995. "Back-propagation neural networks for modeling complex systems". *Artificial Intelligence in Engineering*, Vol. 9, No. 3, pp. 143–151. ISSN 0954-1810. doi:https://doi.org/10.1016/0954-1810(94)00011-S. URL https://www.sciencedirect.com/science/article/pii/095418109400011S.

Hansen, L.S., Pedersen, S. and Durdevic, P., 2019. "Multi-phase flow metering in offshore oil and gas transportation pipelines: Trends and perspectives". *Sensors*, Vol. 19, No. 9. ISSN 1424-8220. doi:10.3390/s19092184. URL https://www.mdpi.com/1424-8220/19/9/2184.

Jia, X., Willard, J., Karpatne, A., Read, J.S., Zwart, J.A., Steinbach, M. and Kumar, V., 2021. "Physics-guided machine learning for scientific discovery: An application in simulating lake temperature profiles". *ACM/IMS Trans. Data Sci.*, Vol. 2, No. 3. ISSN 2691-1922. doi:10.1145/3447814. URL https://doi.org/10.1145/3447814.

Jobson, D.A., 1955. "On the flow of a compressible fluid through orifices". *Proceedings of the Institution of Mechanical Engineers*, Vol. 169, No. 1, pp. 767–776. doi:10.1243/PIME-PROC-1955-169-077-02.

Kanin, E.A., Osiptsov, A.A., Vainshtein, A.L. and Burnaev, E.V., 2019. "A predictive model for steady-state multiphase pipe flow: Machine learning on lab data". *Journal of Petroleum Science and Engineering*, Vol. 180, pp. 727–746. ISSN 09204105. doi:10.1016/j.petrol.2019.05.055.

Karpatne, A., Atluri, G., Faghmous, J.H., Steinbach, M., Banerjee, A., Ganguly, A., Shekhar, S., Samatova, N. and Kumar, V., 2017. "Theory-guided data science: A new paradigm for scientific discovery from data". *IEEE Transactions on Knowledge and Data Engineering*, Vol. 29, No. 10, pp. 2318–2331. doi:10.1109/TKDE.2017.2720168.

Lockhart, R.W. and Martinelli, R.C., 1949. "Proposed correlation of data for isothermal two-phase, two-component flow in pipes". *Chemical Engineering Progress*, Vol. 45, No. 1, pp. 39–48.

Mandhane, J., Gregory, G. and Aziz, K., 1974. "A flow pattern map for gas—liquid flow in horizontal pipes". *International Journal of Multiphase Flow*, Vol. 1, No. 4, pp. 537–553. ISSN 0301-9322. doi:https://doi.org/10.1016/0301-9322(74)90006-8. URL https://www.sciencedirect.com/science/article/pii/0301932274900068.

Minemura, K., Takeoka, T., syoda, S., kazuyuki egasira and yutaka ogawa, 1998. "Correlative mapping method for measuring individual phase flow rates in air-water two-phase flow based on stochastic features". *JSME International Journal Series B*, Vol. 41, No. 4, pp. 863–870. doi:10.1299/jsmeb.41.863.

Murdock, J.W., 1962. "Two-Phase Flow Measurement With Orifices". *Journal of Basic Engineering*, Vol. 84, No. 4, pp. 419–432. ISSN 0021-9223. doi:10.1115/1.3658657. URL https://doi.org/10.1115/1.3658657.

Raissi, M., Perdikaris, P. and Karniadakis, G.E., 2017. "Physics informed deep learning (part i): Data-driven solutions of nonlinear partial differential equations".

Shaban, H. and Tavoularis, S., 2014. "Measurement of gas and liquid flow rates in two-phase pipe flows by the application of machine learning techniques to differential pressure signals". *International Journal of Multiphase Flow*, Vol. 67, pp. 106–117. ISSN 0301-9322. doi:https://doi.org/10.1016/j.ijmultiphaseflow.2014.08.012. URL https://www.sciencedirect.com/science/article/pii/S0301932214001608.

Shah, S., Dey, D., Lovett, C. and Kapoor, A., 2018. "Airsim: High-fidelity visual and physical simulation for autonomous vehicles". In M. Hutter and R. Siegwart, eds., *Field and Service Robotics*. Springer International Publishing, Cham, pp. 621–635. ISBN 978-3-319-67361-5.

Taitel, Y. and Dukler, A.E., 1976. "A model for predicting flow regime transitions in horizontal and near horizontal gas-liquid flow". *AIChE Journal*, Vol. 22, No. 1, pp. 47–55. doi:https://doi.org/10.1002/aic.690220105.

Wang, H., Zhang, M. and Yang, Y., 2020. "Machine learning for multiphase flowrate estimation with time series sensing data". *Measurement: Sensors*, Vol. 10-12, p. 100025. ISSN 2665-9174. doi:https://doi.org/10.1016/j.measen.2020.100025. URL https://www.sciencedirect.com/science/article/pii/S2665917420300222.

Xiang, Z., Peng, W., Zheng, X., Zhao, X. and Yao, W., 2021. "Self-adaptive loss balanced physics-informed neural networks for the incompressible navier-stokes equations". URL http://arxiv.org/abs/2104.06217.

Xie, T., Ghiaasiaan, S. and Karrila, S., 2004. "Artificial neural network approach for flow regime classification in gas–liquid–fiber flows based on frequency domain analysis of pressure signals". *Chemical Engineering Science*, Vol. 59, No. 11, pp. 2241–2251. ISSN 0009-2509. doi:https://doi.org/10.1016/j.ces.2004.02.017.

Zhang, Z., Beck, M.W., Winkler, D.A., Huang, B., Sibanda, W., Goyal, H. and written on behalf of AME Big-Data Clinical Trial Collaborative Group, 2018. "Opening the black box of neural networks: methods for interpreting neural network models in clinical applications". *Annals of Translational Medicine*, Vol. 6, No. 11. ISSN 2305-5847. URL https://atm.amegroups.com/article/view/19682.

7. RESPONSIBILITY NOTICE

The authors are solely responsible for the printed material included in this paper.